

***b*-physics signals of the lightest *CP*-odd Higgs boson in the next-to-minimal supersymmetric standard model at large $\tan\beta$**

Gudrun Hiller*

Ludwig-Maximilians-Universität München, Sektion Physik, Theresienstraße 37, D-80333 München, Germany

(Received 1 May 2004; published 19 August 2004)

We investigate the low energy phenomenology of the lighter pseudoscalar A_1^0 in the NMSSM. The A_1^0 mass can naturally be small due to a global $U(1)_R$ symmetry of the Higgs potential, which is only broken by trilinear soft terms. The A_1^0 mass is further protected from renormalization group effects in the large $\tan\beta$ limit. We calculate the $b \rightarrow s A_1^0$ amplitude at leading order in $\tan\beta$ and work out the contributions to rare K , B and radiative Y decays and B - \bar{B} mixing. We obtain constraints on the A_1^0 mass and couplings and show that masses down to $\mathcal{O}(10)$ MeV are allowed. The b -physics phenomenology of the NMSSM differs from the MSSM in the appearance of sizable renormalization effects from neutral Higgs bosons to the photon and gluon dipole operators and the breakdown of the MSSM correlation between the $B_s \rightarrow \mu^+ \mu^-$ branching ratio and B_s - \bar{B}_s mixing. For A_1^0 masses above the tau threshold the A_1^0 can be searched for in $b \rightarrow s \tau^+ \tau^-$ processes with branching ratios $\lesssim 10^{-3}$.

DOI: 10.1103/PhysRevD.70.034018

PACS number(s): 13.20.He, 13.90.+i, 14.80.Cp

I. INTRODUCTION

Sizable flavor changing neutral current (FCNC) effects in meson decays arise in the minimal supersymmetric standard model (MSSM) at large $\tan\beta$, e.g., [1–6]. In this model, the amplitude of exchanging neutral Higgs bosons between down-type fermions f , i.e. down-type quarks or charged leptons,

$$\sum_{s=h^0, H^0, A^0} \frac{(g_{\bar{f}fs})^2}{m_S^2} \alpha - \frac{\cos^2(\beta-\alpha)}{m_{h^0}^2} - \frac{\sin^2(\beta-\alpha)}{m_{H^0}^2} + \frac{1}{m_{A^0}^2} = 0, \quad (1)$$

vanishes. Here, m_S , $g_{\bar{f}fS}$ denote the Higgs boson masses and couplings to a fermion pair, respectively, and α is the scalar mixing angle. Equation (1) implies that the Wilson coefficients for $b \rightarrow s \ell^+ \ell^-$ decays from scalar and pseudoscalar boson exchange in the MSSM at large $\tan\beta$ are equal with opposite sign [2,3]. If the relation is broken, interesting effects via operator mixing are induced [7]. In particular, the dipole operators responsible for $b \rightarrow s \gamma$ and $b \rightarrow s g$ decays receive sizable contributions from the neutral Higgs bosons. Furthermore, specific contributions to B - \bar{B} mixing from scalar exchange arise. This happens in the presence of more Higgs bosons, such as in the next-to-minimal supersymmetric standard model (NMSSM).

The NMSSM is the MSSM extended by a singlet N , with the superpotential [8,9]

$$W = QY_u H_u U + QY_d H_d D + LY_c H_d E + \lambda H_d H_u N - \frac{1}{3} k N^3. \quad (2)$$

The physical NMSSM Higgs sector consists of three scalars $h^0, H_{1,2}^0$ and two pseudoscalars $A_{1,2}^0$. As in the minimal model, $\tan\beta = v_u/v_d$ denotes the ratio of Higgs doublet vacuum expectation values (VEVs) $v_u = \langle H_u^0 \rangle = v \sin\beta$ and $v_d = \langle H_d^0 \rangle = v \cos\beta$, where $v = \sqrt{2} m_W/g \approx 174$ GeV. The Higgs potential

$$V_{\text{Higgs}} = V_{\text{soft}} + V_F + V_D, \quad (3)$$

where

$$V_{\text{soft}} = m_{H_d}^2 |H_d|^2 + m_{H_u}^2 |H_u|^2 + m_N^2 |N|^2 - (\lambda A_\lambda H_d H_u N + \text{H.c.}) - \left(\frac{1}{3} k A_k N^3 + \text{H.c.} \right), \quad (4)$$

$$V_F = |\lambda|^2 (|H_d|^2 + |H_u|^2) |N|^2 + |\lambda H_d H_u - k N^2|^2, \quad (5)$$

$$V_D = \frac{g^2 + g'^2}{8} (|H_d|^2 - |H_u|^2) + \frac{g^2}{2} |H_u^\dagger H_d|^2, \quad (6)$$

has a global $U(1)_R$ symmetry in the limit of vanishing soft terms $A_k, A_\lambda \rightarrow 0$ [10]. If this symmetry is broken only slightly, the model naturally contains a light pseudoscalar. Its mass is given as

$$m_{A_1^0}^2 = 3 k x A_k + \mathcal{O}\left(\frac{1}{\tan\beta}\right) \quad (7)$$

where $x = \langle N \rangle$ denotes the VEV of the singlet. Note that a small A_k remains small under renormalization group running and thus protects $m_{A_1^0}$.

Lower bounds on CP -odd scalar masses are not very stringent and can be as low as ~ 100 MeV [11]. Since the coupling $h^0 A_1^0 A_1^0$ is not suppressed, the scalar Higgs boson

*Email address: hiller@theorie.physik.uni-muenchen.de

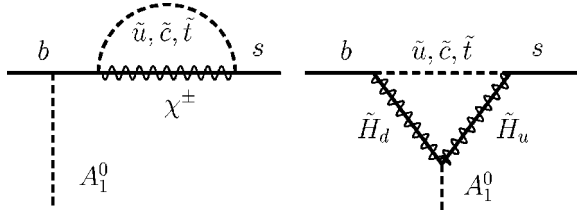


FIG. 1. The leading $b \rightarrow s A_1^0$ diagrams at large $\tan \beta$ in the NMSSM.

predominantly decays into lighter pseudoscalars. This has important consequences for the Tevatron and LHC Higgs boson searches [10,12].

The motivation for this work is to find out how and to what extent the NMSSM would signal itself in rare b decays and, at the same time, whether existing data provide already bounds on the NMSSM parameter space. We employ the large $\tan \beta \geq 30$ and small $A_k \ll m_w, x$ limit and no flavor or CP violation other than in the CKM matrix (“minimal flavor violation”). Since a small A_λ is not stable under radiative corrections, we do not expand in small A_λ and keep it finite. Our study is based on mostly generic features of the NMSSM. Specific analyses of the NMSSM particle spectrum and parameter space have been carried out in a grand unified theory (GUT) framework [13] at large $\tan \beta$ [14], with gauge mediated SUSY breaking [15] and with anomaly mediation [16]. For Higgs boson production in rare b decays in other models, see e.g., [17,18].

This paper is organized as follows: In Sec. II we calculate the amplitude for $b \rightarrow s A_1^0$ decays at large $\tan \beta$. We discuss the NMSSM parameter space in Sec. III. Phenomenological bounds from FCNC decays, B - \bar{B} mixing and Y decays are worked out in Sec. IV. In Sec. V we investigate the impact on semileptonic and radiative rare b decays. We also analyze how much the MSSM tree level relation, Eq. (1), is broken by loop corrections. We conclude in Sec. VI. Feynman rules and the NMSSM particle spectrum at large $\tan \beta$ and auxiliary functions are given in Appendixes A and B. In Appendix C we give decay rates of the A_1^0 and b -decay branching ratios.

II. $b \rightarrow s A_1^0$ AMPLITUDE AT LARGE $\tan \beta$

The amplitude for a FCNC $b \rightarrow s$ transition into the lightest CP -odd scalar A_1^0 in the NMSSM is induced at one loop. In the large $\tan \beta$ limit, only two diagrams remain to be calculated, which are shown in Fig. 1. (We neglect the strange quark mass.) Feynman rules are given in Appendix A 1; see also [19] for the MSSM and [20] for the NMSSM.

The stop chargino wave function correction is identical to the corresponding one in the MSSM. Since the coupling of the A_1^0 to down-type fermions is of the order of $(\tan \beta)^0$, the one-particle reducible (1PR) diagram contributes to the $b \rightarrow s A_1^0$ amplitude at order $\tan \beta$. The vertex correction shown in Fig. 1 is the only 1PI diagram linear in $\tan \beta$ because (i) the $H^\pm W^\mp A_1^0$ coupling is $1/\tan \beta$ suppressed since the A_1^0 is predominantly the gauge singlet (the $H^+ H^- A_1^0$, $W^+ W^- A_1^0$ vertices are forbidden by CP), (ii) the coupling of the A_1^0 to

up-type quarks is $1/\tan^2 \beta$, (iii) the coupling of the A_1^0 to up-type squarks is $1/\tan \beta$ which can be seen from the F-term contribution $|\partial W/\partial H_u|^2$ and (iv) the only $\tan \beta$ enhancement comes from the $b_R \tilde{t}_L \tilde{H}_d$ or $b_R t_L H_d$ vertices.

We obtain the amplitude

$$i\mathcal{A}(b \rightarrow s A_1^0) = -4 \frac{G_F}{\sqrt{2}} V_{tb} V_{ts}^* C_A \frac{1}{16\pi^2} \bar{s}_L b_R A_1^0 \quad (8)$$

where

$$C_A = -i \frac{\tan \beta m_b}{\sqrt{2}} \left[-\frac{\delta_-}{x} \sum_{i=1,2} X_i + \lambda m_t \sin \theta_{\tilde{t}} \cos \theta_{\tilde{t}} \sum_{l,j=1,2} Y_{lj} \right] \quad (9)$$

and δ_- parametrizes the $A_1^0 \bar{b} b$ coupling; see Eq. (A4). The X, Y terms in Eq. (9) result from the wave function and vertex correction, respectively. They are written as

$$X_i = m_{\chi_i} U_{i2} \left\{ \sqrt{2} m_w V_{i1} [-D_3(y_{c,i}) + D_3(y_{l,i}) \cos^2 \theta_{\tilde{t}} + D_3(y_{2,i}) \sin^2 \theta_{\tilde{t}}] - m_t V_{i2} \sin \theta_{\tilde{t}} \cos \theta_{\tilde{t}} [D_3(y_{1,i}) - D_3(y_{2,i})] \right\}, \quad (10)$$

$$Y_{lj} = V_{j2} U_{l2} \left[\left(y_{1j} U_{j2} V_{l2} - \frac{m_{\chi_l}}{m_{\chi_j}} U_{l2} V_{j2} \right) D_2(y_{1j}, z_{lj}) - \left(y_{2j} U_{j2} V_{l2} - \frac{m_{\chi_l}}{m_{\chi_j}} U_{l2} V_{j2} \right) D_2(y_{2j}, z_{lj}) \right] \quad (11)$$

where

$$y_{kj} = \frac{m_{\tilde{t}_k}^2}{m_{\chi_j}^2}, \quad y_{cj} = \frac{m_{\tilde{c}}^2}{m_{\chi_j}^2}, \quad z_{lj} = \frac{m_{\chi_l}^2}{m_{\chi_j}^2} \quad (12)$$

and $m_{\tilde{t}_k}, m_{\tilde{c}}, m_{\chi_l}$ denote the stop, scharm and chargino masses. The stop mixing angle $\theta_{\tilde{t}}$, the chargino mixing matrices U, V and the loop functions D_2, D_3 are defined in Appendix B. We used unitarity of the Cabibbo-Kobayashi-Maskawa (CKM) matrix and neglected squark mixing other than for stops and mass splitting between the first two generations. The $b \rightarrow d A_1^0$ amplitude is obtained by replacing s by d everywhere in Eq. (8). The $s \rightarrow d A_1^0$ amplitude is given correspondingly with also changing m_b to m_s in Eq. (9). Note that our calculation holds for $|\delta_{\pm} v/x| < \tan \beta$; see Appendix A. e.g., for larger values of $\delta_{\pm} v/x$ the A_1^0 loses its mostly singlet nature and more $b \rightarrow s A_1^0$ diagrams need to be calculated.

The coupling C_A vanishes if the super Glashow-Iliopoulos-Maiani (GIM) mechanism is active, that is if either all squark masses are degenerate or $m_{\tilde{c}} = m_{\tilde{t}_1}$ and $\theta_{\tilde{t}} = 0$ (or π) or $m_{\tilde{c}} = m_{\tilde{t}_2}$ and $\theta_{\tilde{t}} = \pi/2$. We estimate the generic size of C_A with order one stop mixing as

$$|C_A| \simeq \mathcal{O}\left(\delta_- \tan \beta m_b m_t \frac{m_\chi}{x}\right) + \mathcal{O}(\lambda \tan \beta m_b m_t). \quad (13)$$

Since λx is the NMSSM μ term which sets the mass scale for the charginos, both terms are of comparable size.

III. VIABLE POINTS IN THE NMSSM PARAMETER SPACE

The relevant NMSSM parameter space consists of λ, k from the superpotential, the soft breaking terms A_λ, A_k , the gaugino mass m_2 , stop and scharm masses, the stop mixing angle $\theta_{\tilde{t}}$ and $\tan \beta$. We evaluate all parameters at the electroweak scale.

The dimensionless couplings λ and k run towards smaller values, e.g., $\lambda^2 + k^2 \leq 0.6$ at the electroweak scale for $\lambda, k \leq 2\pi$ at the high, GUT scale [21]. We use $|\lambda|, |k| \leq 1$. Similar to the MSSM, electroweak symmetry breaking at large $\tan \beta$ requires [14]

$$m_{H_u}^2 = -(\lambda x)^2 - \frac{m_Z^2}{2} \quad (14)$$

and therefore the product of λ and x should not exceed $\sim \mathcal{O}(1)$ TeV to avoid fine-tuning. On the other hand, the chargino mass scale is driven by λx , which should be at least $\mathcal{O}(100)$ GeV by experimental search limits. We assume the singlet VEV x to be of the order of the Fermi scale v , or at least not smaller than 100 GeV and not bigger than 3 TeV. If x exceeds this value, its relation to the other VEVs becomes unnatural and the model does not give a solution to the μ problem [8]. Hence, the size of λ is bounded from below as $|\lambda| \geq \text{few} \times 10^{-2}$ [15,21]. Further, the extremization condition

$$m_{H_d}^2 = -\lambda^2(x^2 + v^2) + m_A^2 + \frac{m_Z^2}{2} \quad (15)$$

where we defined

$$m_A^2 \equiv \lambda(A_\lambda + kx)x \tan \beta \quad (16)$$

implies some cancellation among the $\tan \beta$ enhanced terms as [14]

$$A_\lambda + kx \sim \frac{\mathcal{O}(100-1000 \text{ GeV})}{\tan \beta}. \quad (17)$$

Note that m_A sets the scale for the heavy Higgs bosons A_2^0, H_2^0 and H^\pm ; see Appendix A.

The NMSSM is further constrained by non-observation of Higgs bosons and superpartners. At large $\tan \beta$, the mass of the lightest scalar at tree level is given as

$$m_{h^0}^2 \simeq m_Z^2 - \frac{\lambda^4 v^2}{k^2} \quad (18)$$

where we expanded Eq. (A7) in $m_Z^2/4k^2x^2 \ll 1$ and $\lambda^2 v/k^2x \ll 1$. In this approximation also $m_{H_1^0}^2 \simeq 4k^2x^2 + \lambda^4 v^2/k^2$ and the scalar mixing angle θ is small. Like in the MSSM, the h^0

tree level mass cannot be bigger than the Z mass because the raising of its upper bound in the NMSSM is suppressed by large $\tan \beta$. To be phenomenologically viable, m_{h^0} has to be lifted by radiative corrections above the current search limit as in the MSSM [22]. We require the scalar tree level mass to be bigger than 89 GeV, which favors small λ or λ/k less than 1. We allow for $|m_2| \leq 1$ TeV and check that the charginos are heavier than 90 GeV. We treat the pseudoscalar masses $m_{A_1^0}$ and $m_{A_2^0}$ with $m_{A_2^0} \geq 130$ GeV as free parameters, i.e. adjust A_k and A_λ accordingly. The squark masses and stop mixing angle are effective parameters with $m_{\tilde{t}_1} > 90$ GeV and $m_{\tilde{t}_2}, m_{\tilde{c}} \sim 1$ TeV and we do not relate them to fundamental parameters in the Lagrangian.

The down-type fermion- A_1^0 vertex is proportional to $\delta_- v/x$; see Eq. (A9). From Eqs. (16) and (17) we obtain

$$\frac{v}{x} \delta_- = \frac{v}{x} \left[-3 \frac{k\lambda x^2}{m_A^2} \tan \beta + 1 \right] \simeq \pm 3 \frac{kv m_\chi}{m_A^2} \tan \beta \quad (19)$$

where the second equation is a good approximation for not too large $m_A \lesssim 500$ GeV. It then gives a lower bound on $|\delta_- v/x|$. In particular, for $\tan \beta = 30$, $m_A \lesssim 500$ (200) (130) GeV and the ranges of parameters given in the preceding paragraphs, we obtain $|\delta_- v/x| \geq 0.1$ (1)(3). For larger values of m_A cancellations between the two terms in Eq. (19) are possible. Note that the $\tan \beta$ factor is only a formal enhancement, since it is canceled by the one in m_A^2 . We find that $|\delta_- v/x| \leq 62$ (16) for $m_A \geq 500$ (1000) GeV. Note that the small $A_\lambda \ll kx$ limit with $\delta_- \simeq -2$ makes its hard to satisfy Eq. (17).

IV. PHENOMENOLOGY OF THE LIGHT A_1^0

We work out constraints on the mass of the A_1^0 in the NMSSM at large $\tan \beta$ from A_1^0 production in rare decays (Sec. IV A), \bar{B} - B mixing (Sec. IV B) and $B_s \rightarrow \mu^+ \mu^-$ decays (Sec. IV C). We make use of the $b \rightarrow s A_1^0$ amplitude calculated in Sec. II. We scan the parameter space in the regions discussed in Sec. III. All FCNC bounds can be evaded by a sufficiently tuned-in super GIM mechanism; see Sec. II. To quantify this, we demand in our numerical analysis for the mass splitting $m_{\tilde{t}_2} - m_{\tilde{t}_1} > 50$ GeV while varying $m_{\tilde{t}_1}$ and for the stop mixing $\epsilon < \theta_{\tilde{t}} < \pi/2 - \epsilon$ or $\pi/2 + \epsilon < \theta_{\tilde{t}} < \pi - \epsilon$ with $\epsilon = 0.05$. Bounds from other processes are discussed in Sec. IV D.

Many experimental constraints we use here apply only if the A_1^0 is sufficiently stable, i.e., leaves the detector as missing energy. This happens if the pseudoscalar width is smaller than $E_A/(m_{A_1^0} d)$, where $d \sim \mathcal{O}(10)$ m is the size of the detector and E_A the A_1^0 energy in the laboratory frame. We work out bounds on $m_{A_1^0}$ as a function of $|\delta_- v/x|$. If this coupling gets smaller, the pseudoscalar decay rate decreases, and a heavier Higgs boson will become missing energy and vice versa. For decay rates of the A_1^0 , see Appendix C.

For Higgs boson masses below $2m_\mu$ only the $e^+ e^-$ and $\gamma\gamma$ decay channels are relevant. (The $A_1^0 \rightarrow \pi^0 \gamma$ decay is

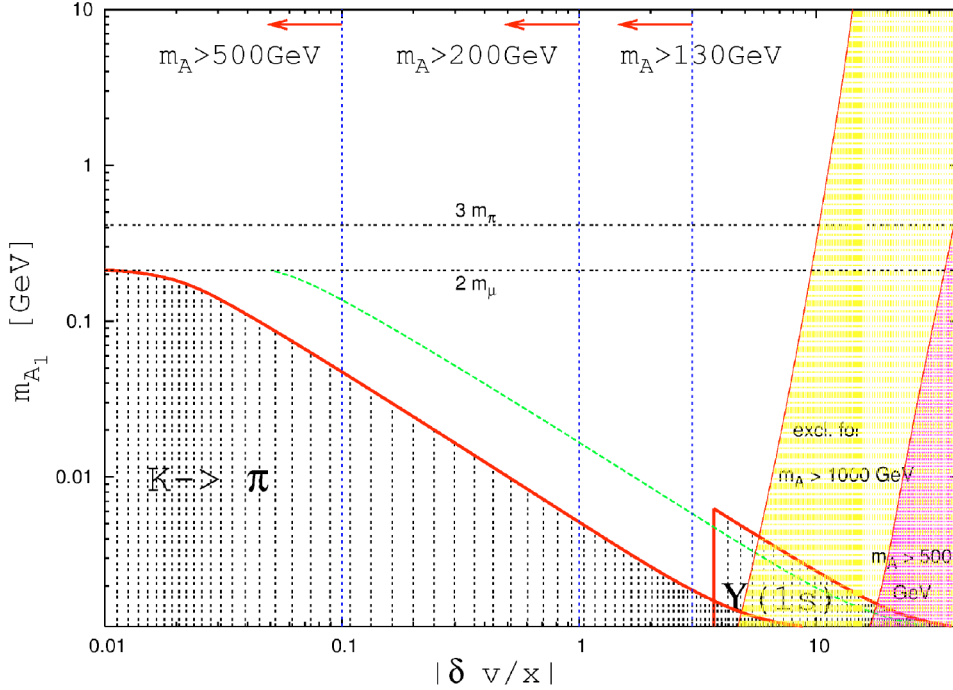


FIG. 2. Constraints on the A_1^0 mass as a function of $|\delta_{-v/x}|$ at $\tan\beta=30$ in the NMSSM. Shaded regions are excluded. The left bottom corner is excluded by rare K decay; see Eq. (21). The triangular region to the lower right is obtained from radiative $Y(1s)$ decays; see Eq. (35). The region to the left of the vertical dashed blue lines can only be reached if m_A is bigger than the value indicated; see Sec. III. Constraints from Δm_d are given for $m_A \geq 500$ GeV and $m_A \geq 1000$ GeV. We also show the missing energy condition for $B \rightarrow K$ decays given in Eq. (20) (dashed green line). The vertical dashed lines indicate $m_{A_1^0} = 2m_\mu$ and $3m_\pi$.

forbidden by CP and angular momentum conservation and the $A_1^0 \rightarrow \pi^0 \gamma \gamma$ decay is suppressed with respect to the dielectron mode by phase space and powers of α .) The $\gamma \gamma$ mode can compete with $A_1^0 \rightarrow f\bar{f}$ decays only near the dimuon threshold. This weakens the missing energy bounds in that region.

The point we want to make is to show that in the NMSSM A_1^0 masses in the GeV range and below are not ruled out. This is summarized in Fig. 2. For details see the following subsections. All experimental bounds are taken at the 90% confidence level. The requisite $b \rightarrow A_1^0$ branching ratios are given in Appendix C. We recall that our approximation breaks down if $|\delta_{\pm v/x}|$ approaches $\tan\beta$.

A. Rare K and B decays

If the Higgs boson is light enough, it can be produced in $b \rightarrow s A_1^0$ or $s \rightarrow d A_1^0$ processes. We analyze what bounds exist depending on the mass of the A_1^0 .

1. $2m_e < m_{A_1^0} < 2m_\mu$

When produced in rare B -meson decays the A_1^0 decays outside of the detector if

$$m_{A_1^0} \leq 17 \text{ MeV} / |\delta_{-v/x}|. \quad (20)$$

In this region the CLEO bound $\mathcal{B}(B \rightarrow K_s^0 X^0) < 5.3 \times 10^{-5}$ [23] applies. There is a similar missing energy bound from BaBar $\mathcal{B}(B^- \rightarrow K^- \nu \bar{\nu}) < 7.0 \times 10^{-5}$ [24].¹ We find that masses in the range given in Eq. (20) are disfavored since the

¹The experimental cut on the K momentum $|\vec{p}_K| > 1.5$ GeV is no restriction for light $m_{A_1^0} \ll m_B$ discussed here.

$B \rightarrow K A_1^0$ decay [see Eq. (C5)] would happen too rapidly for most of the parameter space, although cannot rigorously be excluded. We stress that the size of the coupling C_A can be quite large [see Eq. (13)] and already $\mathcal{B}(B \rightarrow X_s A_1^0) < 1$ cuts out a fraction of NMSSM points.

Rare decays into e^+e^- constrain Higgs boson masses below the muon threshold. However, the measurements of the inclusive $B \rightarrow X_s e^+e^-$ branching ratios contain cuts on the di-lepton mass $m_{ee} \geq 2m_\mu$ [25,26]. In the analysis of $B \rightarrow K^{(*)} e^+e^-$ decays Belle applies $m_{ee} > 0.14$ GeV [27], whereas BaBar [28] has no cut, but the efficiency is low in that region due to conversion photons. Likewise, measurements of $K^+ \rightarrow \pi^+ e^+e^-$ decays employ a high mass trigger [29]. Since also close to $2m_\mu$ the two-photon decay of the A_1^0 becomes sizable, we do not take the e^+e^- data into account.

The bound $\mathcal{B}(K^+ \rightarrow \pi^+ A_1^0) < 4.5 \times 10^{-11}$ [30] is applicable if the A_1^0 becomes sufficiently stable to escape the detector. This happens for masses

$$m_{A_1^0} \leq 5 \text{ MeV} / |\delta_{-v/x}| \quad (21)$$

which then are excluded. The K -decay bound is five orders of magnitude better than the one from $B \rightarrow K$ decays, because the CKM and mass suppression of the $K \rightarrow \pi A_1^0$ decay rate is compensated by the difference in lifetime $|V_{td}/V_{ts}|^2 (m_K/m_B)^3 \tau(K^+)/\tau(B^+) \approx 0.24$ [31]; see Eq. (C5) and its $K \rightarrow \pi$ counterpart.

2. $2m_\mu < m_{A_1^0} < 2m_\tau$

A_1^0 decays into a muon pair are included in $B \rightarrow X_s \mu^+ \mu^-$ signals. Comparison of the $B \rightarrow X_s A_1^0$ branching ratio [see Eq. (C4)] with the data $\mathcal{B}(B \rightarrow X_s \mu^+ \mu^-) \leq 10.4 \times 10^{-6}$ [7,25,26] shows that this is very unlikely. The same happens in $K \rightarrow \pi \mu^+ \mu^-$ decays, which for $m_{A_1^0} < m_K - m_\pi$

can hide a pseudoscalar decaying into muons. With $\mathcal{B}(K^+ \rightarrow \pi^+ \mu^+ \mu^-) \leq 10.4 \times 10^{-8}$ [31] only a tiny number of points survives the scan. All allowed points are at the GIM boundary $\theta_{\tilde{\tau}} \approx \pi/2$, which is set by our value of the cutoff ϵ .

Above the 3π threshold sizable hadronic decays open up. (The $A_1^0 \rightarrow 2\pi\gamma$ decay is suppressed with respect to the dimuon channel by phase space and α , whereas $A_1^0 \rightarrow 2\pi$ decay is forbidden by *CP* invariance.) For the A_1^0 decaying hadronically into a strange final state we use $\mathcal{B}(b \rightarrow sg) < 9\%$ [32]. This thins out the NMSSM model space for $3m_\pi < m_{A_1^0} < 2m_\tau$, but cannot exclude this region. [We use $\mathcal{B}(b \rightarrow sA_1^0) > \mathcal{B}(b \rightarrow dA_1^0)$.]

$$3. 2m_\tau < m_{A_1^0} \leq m_B$$

If the A_1^0 is above the tau threshold, most of the time it decays into $\tau^+ \tau^-$ because its coupling to $c\bar{c}$ is $\tan^2\beta$ suppressed. Similar to the constraint on the hadronically decaying pseudoscalar (see Sec. IV A 2, the mildly model-dependent bound $\mathcal{B}(B \rightarrow X_s \tau^+ \tau^-) < 5\%$ [33] is not a challenge to the light *CP*-odd Higgs scenario.

B. NMSSM neutral Higgs contributions to B - \bar{B} mixing

We calculate the contribution to B - \bar{B} mixing from pseudoscalar $A_{1,2}^0$ and scalar $h^0, H_{1,2}^0$ Higgs boson exchange in the NMSSM at large $\tan\beta$. It arises at two loop order from double insertion of the FCNC $\bar{s}b$ -Higgs vertices such as generated by the diagrams in Fig. 1 for the A_1^0 and an intermediate boson propagator. The dominant diagrams induced by the heavy Higgs bosons; i.e., the ones other than the lightest *CP*-odd scalar are the wave function corrections contributions with A_2^0, H_2^0 exchange—see the Feynman rules in Appendix A 1. They can compete with one-loop contributions such as the standard model (SM) box diagrams due to their $\tan^4\beta$ enhancement. Contributions from h^0, H_1^0 are subleading in $\tan\beta$. We use an effective Hamiltonian ($q=d,s$)

$$\mathcal{H}_{eff}^{\Delta B=2} = \frac{G_F^2 m_W^2}{16\pi^2} (V_{tb} V_{tq}^*)^2 \sum_i C_i \mathcal{Q}_i \quad (22)$$

where some of the relevant operators are written as (see, e.g., [6])

$$\mathcal{Q}^{VLL} = (\bar{q}_L \gamma_\mu b_L) (\bar{q}_L \gamma^\mu b_L), \quad (23)$$

$$\mathcal{Q}_1^{SRR} = (\bar{q}_L b_R) (\bar{q}_L b_R), \quad (24)$$

$$\mathcal{Q}_1^{SLR} = (\bar{q}_R b_L) (\bar{q}_L b_R). \quad (25)$$

The SM contribution is in the coefficient C^{VLL} . The A_2^0, H_2^0 masses are degenerate at large $\tan\beta$ and their respective contributions to \mathcal{Q}_1^{SRR} cancel each other just like in the MSSM; see Eq. (1). They do, however, contribute to the operator \mathcal{Q}_1^{SLR} at order m_q/m_b , and are important for B_s mesons. [This is the well-known double penguin (DP) contribution of the MSSM [5,6].]

We obtain, at order $\tan^2\beta/m_{A_1^0}^2$ in the NMSSM from A_1^0 boson exchange,

$$C_1^{SRR}(\mu_t) = -\frac{1}{4\pi^2} \frac{C_A^2}{m_W^2 m_{A_1^0}^2} \quad (26)$$

at the high, electroweak (matching) scale μ_t . Finite widths effects are neglected. We define the size of the $B_q - \bar{B}_q$ mass difference Δm_q with respect to its SM value as

$$\frac{\Delta m_q}{(\Delta m_q)_{SM}} = 1 + f_q \quad (27)$$

where

$$f_q = \frac{\bar{P}_1^{SLL}}{S_0(\mu_t)} C_1^{SRR}(\mu_t) \quad (28)$$

and $S_0(\mu_t) = 2.38$ and $\bar{P}_1^{SLL} = -0.37$ [6]. In Eq. (28) the NMSSM contribution to Δm_d by neutral Higgs boson exchange in the $m_q = 0$ limit has been given. To be in agreement with data we require $f_d > -0.6$ (f_d is negative). This includes 20% uncertainty and allows for cancellations between the A_1^0 contribution and the charged Higgs bosons, chargino boxes and the double penguins. We assume similar sizes as in the MSSM, where $-0.2 \leq f_d^{H^\pm} + f_d^{X^\pm} + f_d^{DP} \leq 0.4$ [6]. We find constraints for larger values of $|\delta_{-v}/x|$ and $m_A \geq 500$ GeV, which are displayed in Fig. 2 for $\tan\beta = 30$. The other branch with $1 + f_d < 0$, where the NMSSM correction is larger than the SM box gives very similar constraints and is not shown. The leading A_1^0 contribution to B - \bar{B} mixing is universal in minimal flavor violation, $f_d = f_s$, since we neglect light quark masses.

C. $B_s \rightarrow \mu^+ \mu^-$ decays

We work out the contributions to $B_s \rightarrow \mu^+ \mu^-$ decays from neutral Higgs boson exchanges in the large $\tan\beta$ limit of the NMSSM. With the effective Hamiltonian

$$\mathcal{H}_{eff} = -\frac{G_F}{\sqrt{2}} V_{tb} V_{ts}^* \sum_i C_i \mathcal{O}_i \quad (29)$$

where

$$\mathcal{O}_S = \frac{e^2}{16\pi^2} \bar{s}_L b_R \bar{\ell} \ell, \quad \mathcal{O}_P = \frac{e^2}{16\pi^2} \bar{s}_L b_R \bar{\ell} \gamma_5 \ell, \quad (30)$$

we obtain, at the electroweak scale (in parentheses is given the particle that induces a particular Wilson coefficient),

$$C_S = C_S(H_2^0) = -C_P(A_2^0), \quad C_P = C_P(A_1^0) + C_P(A_2^0) \quad (31)$$

where

$$C_P(A_1^0) = m_b m_\ell \tan \beta \frac{v}{4m_W^2 \sin^2 \theta_W} \left(\frac{v \delta_-}{x} \right) \frac{1}{m_{B_s}^2 - m_{A_1^0}^2} \times \left[-\frac{\delta_-}{x} \sum_{i=1,2} X_i + \lambda m_i \sin \theta_i \cos \theta_i \sum_{l,j=1,2} Y_{lj} \right], \quad (32)$$

$$C_P(A_2^0) = m_b m_\ell \tan^3 \beta \frac{1}{4m_A^2 m_W^2 \sin^2 \theta_W} \sum_{i=1,2} X_i. \quad (33)$$

The expressions for X and Y are given in Sec. II. Our result for the A_2^0, H_2^0 contributions agrees with the corresponding MSSM calculations [3]. Note that the contributions from A_2^0 and H_2^0 are equal with opposite sign. Similar to $B-\bar{B}$ mixing discussed in Sec. IV B, the scalars h^0 and H_1^0 contribute at subleading order in $\tan \beta$.

The coefficients $C_{S,P}$ are model independently constrained by data on the $B_s \rightarrow \mu^+ \mu^-$ branching ratio. With $\mathcal{B}(B_s \rightarrow \mu^+ \mu^-) < 5.8 \times 10^{-7}$ [34] we obtain, at the scale $\mu = m_W$,

$$\sqrt{|C_S|^2 + |C_P + \delta_{10}|^2} \leq 1.3 \left[\frac{\mathcal{B}(B_s \rightarrow \mu^+ \mu^-)}{5.8 \times 10^{-7}} \right]^{1/2} \left[\frac{238 \text{ MeV}}{f_{B_s}} \right]. \quad (34)$$

Here, δ_{10} stems from the operator $\mathcal{O}_{10} \propto \bar{s}_L \gamma_\mu b_L \bar{\ell} \gamma^\mu \gamma_5 \ell$, see [7] for details. We find with $\delta_{10}^{SM} = -0.095$,² at $\tan \beta = 30$, the upper limits $|\delta_- v/x| \leq 42(16)$ for $m_A = 500(1000)$ GeV, which are weaker than the corresponding Δm_d ones. The expressions for the CKM suppressed $B_d \rightarrow \mu^+ \mu^-$ decay are readily obtained. Its experimental constraint is not as good as the B_s one, but we can cut out both $m_{A_1^0} \approx m_{B_d}$ and $m_{A_1^0} \approx m_{B_s}$.

D. Non-FCNC bounds

The bounds from radiative Y decays apply if the A_1^0 leaves the detector unseen [31,36]. As a result of the larger boost, the critical width to do so is larger than in B -meson decays by m_Y/m_B . We use $\mathcal{B}(Y(1s) \rightarrow A^0 \gamma) < 1.3 \times 10^{-5}$ [36] and obtain, with Eq. (C7),

$$|\delta_- v/x| \leq 3.7 \quad \text{for } m_{A_1^0} \leq 23 \text{ MeV} / |\delta_- v/x| < 2 m_\mu. \quad (35)$$

Furthermore, we get an upper bound $|\delta_- v/x| \leq 100$ from $\mathcal{B}(Y(1s) \rightarrow A_1^0 \gamma) < 1$.

Mass bounds from hadronic collisions are not better than few to 200 MeV and astrophysics gives $m_{A_1^0} \geq 0.2$ MeV [31], which contain some model dependence.

²Supersymmetry (SUSY) effects are not $\tan \beta$ enhanced in \mathcal{O}_{10} and are small with minimal flavor violation [35].

V. IMPLICATIONS FOR $b \rightarrow s \ell^+ \ell^-$ AND $b \rightarrow s \gamma, g$

Similar to the operators $\mathcal{O}_{S,P}$ discussed in Sec. IV C, the NMSSM Higgs sector also induces contributions to 4-fermion operators with quarks and leptons (f denotes a fermion)

$$\mathcal{O}_L^f = \bar{s}_L b_R \bar{f}_R f_L, \quad \mathcal{O}_R^f = \bar{s}_L b_R \bar{f}_L f_R \quad (36)$$

where

$$C_{L,R}^f = \frac{e^2}{16\pi^2} \frac{m_f}{m_\mu} (C_{S^\mp} C_P). \quad (37)$$

These couplings arise in the NMSSM at large $\tan \beta$, where

$$C_S - C_P = -2C_P(A_2^0) - C_P(A_1^0), \quad C_S + C_P = C_P(A_1^0). \quad (38)$$

This is different from the MSSM, where the A_1^0 contribution is absent and the sum of C_S and C_P and hence C_R^f vanish. We discuss corrections to this tree level statement in Sec. V A. All Wilson coefficients refer to the Hamiltonian in Eq. (29) and are evaluated at the scale $\mu = m_W$ unless otherwise stated.

The constraint given in Eq. (34) implies, for the Wilson coefficients for b quarks (we update the findings of Ref. [7] with the improved $B_s \rightarrow \mu^+ \mu^-$ bound [34]),

$$\sqrt{|C_L^b|^2 + |C_R^b|^2} \leq 0.03. \quad (39)$$

The operators $\mathcal{O}_{L,R}^b$ enter radiative and semileptonic rare $b \rightarrow s$ decays at one loop [7,37]. With the bound in Eq. (39) the new physics effect from \mathcal{O}_L^b is small, at the percent level [7]. However, the renormalization effect induced at leading log by \mathcal{O}_R^b can be large for the photon and gluon dipole operators \mathcal{O}_7 and \mathcal{O}_8 , which can be written as

$$\mathcal{O}_7 = \frac{e}{16\pi^2} m_b \bar{s}_L \sigma_{\mu\nu} b_R F^{\mu\nu},$$

$$\mathcal{O}_8 = \frac{g_s}{16\pi^2} m_b \bar{s}_L \alpha \sigma_{\mu\nu} T_{\alpha\beta}^a b_R G^{a\mu\nu}. \quad (40)$$

To be specific, we normalize their coefficients to the ones in the SM, and denote this ratio by ξ , such that $\xi^{SM} = 1$. With (see [7] for details)

$$\xi_7(m_b) = 0.514 + 0.450 \xi_7(m_W) + 0.035 \xi_8(m_W) - 2.319 C_R^b, \quad (41)$$

$$\xi_8(m_b) = 0.542 + 0.458 \xi_8(m_W) + 19.790 C_R^b \quad (42)$$

and Eq. (39) corrections of up to 7% and 59% to ξ_7 and ξ_8 are possible. This has impact on the extraction of Wilson coefficients in $b \rightarrow s \gamma$, $b \rightarrow s g$ and $b \rightarrow s \ell^+ \ell^-$ decays [7]. For a full analysis of these decays, also the matching contributions to $C_{7,8}$ from neutral Higgs loops in the large $\tan \beta$ NMSSM have to be calculated. Note that $\tan \beta$ enhanced

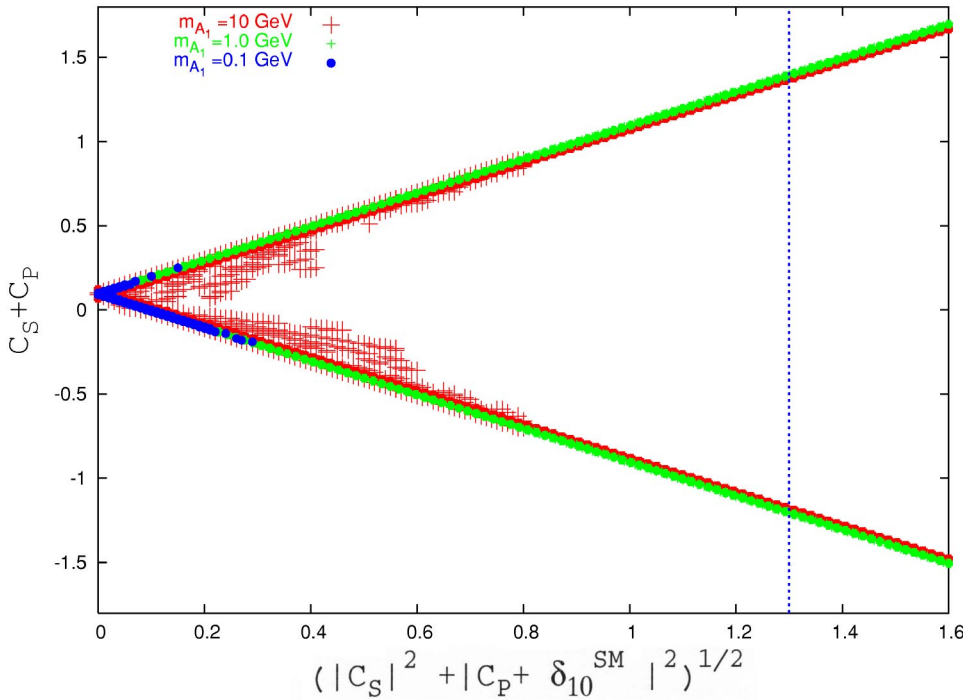


FIG. 3. The correlation between $C_S + C_P$ and $\sqrt{|C_S|^2 + |C_P + \delta_{10}^{SM}|^2}$ in the NMSSM for $\tan \beta = 30$, $m_A = 500$ GeV and $m_{A_1^0} = 0.1, 1$ and 10 GeV. Also shown is the experimental upper bound given in Eq. (34) (dashed line).

corrections to the *b*-quark mass, CKM elements and FCNCs from non-holomorphic terms arise [1,5,6]. We leave this for future work.

A. Estimates of $C_S + C_P$ and C_R^b

We work out the NMSSM reach in $C_S + C_P$ by taking into account all constraints discussed in the previous Secs. III and IV. The value of $C_S + C_P$ can saturate its upper bound given in Eq. (34) for large ranges of the parameter space. If the A_1^0 gets very light, however, the $b \rightarrow s A_1^0$ coupling C_A has to decrease and $C_S + C_P$ is small; e.g., for $m_{A_1^0} = 10$ MeV is $|C_S + C_P| \leq 0.06$. For intermediate masses the A_1^0 contribution dominates over the one from the heavy pseudoscalar, that is $|C_P| \gg |C_S|$ and $|C_R^b| \approx |C_L^b| \leq 0.024$. This is illustrated in Fig. 3, where we show $C_S + C_P$ as a function of $\sqrt{|C_S|^2 + |C_P + \delta_{10}^{SM}|^2} \propto \sqrt{\mathcal{B}(B_s \rightarrow \mu^+ \mu^-)}$ [see Eq. (34)] for $m_A = 500$ GeV and different values of $m_{A_1^0}$.

In the MSSM the size of $C_S + C_P$ is driven by the relation Eq. (1), which is not protected from radiative corrections. To study their size we employ the two-loop calculation encoded in FEYNHIGGS v. 2.02 [38]. By scanning the MSSM parameter space we find

$$\left| \frac{C_S + C_P}{C_S - C_P} \right|_{MSSM} < 0.2$$

or

$$|C_S + C_P|_{MSSM} < 0.08$$

and

$$|C_R^b|_{MSSM} < 1.3 \times 10^{-3}. \tag{43}$$

The smallness of $C_S + C_P$ is a feature of the Higgs sector of the MSSM. It holds also with flavor violation beyond the CKM matrix. As a result, the logarithmic renormalization of the dipole operators from neutral (pseudo)scalars is tiny in this model. For example, consider additional right handed currents, which induce contributions to the helicity flipped operators \mathcal{O}'_i , i.e. the ones obtained from \mathcal{O}_i with right *R* and left *L* chiralities interchanged. In this case, $C'_S - C'_P$ mixes onto the flipped dipole operators $\mathcal{O}'_{7,8}$, but $C'_S = C'_P$ in the large $\tan \beta$ MSSM [5].

VI. CONCLUSIONS

We investigated the phenomenology of the light pseudo-scalar A_1^0 which lives in the NMSSM spectrum at large $\tan \beta$. The A_1^0 has suppressed gauge interactions but couples to Higgs bosons and down-type matter. We calculated the $b \rightarrow s A_1^0$ amplitude at leading order in $\tan \beta$. Based on this, we estimated the NMSSM contributions to rare *K*, *B* and radiative Υ decays with the A_1^0 in the final state, $B_s \rightarrow \mu^+ \mu^-$ decays and *B*- \bar{B} mixing. We showed that low energy data provide constraints on the A_1^0 mass and couplings, but leave masses down to $\mathcal{O}(10)$ MeV viable; see Fig. 2. The A_1^0 predominantly decays into $\tau^+ \tau^-$ for $2m_\tau < m_{A_1^0} < 2m_b$, light hadrons for $3m_\pi < m_{A_1^0} < 2m_\tau$ and $e^+ e^-$ or $\gamma\gamma$ for $2m_e < m_{A_1^0} < 2m_\mu$. In the latter range, the A_1^0 can live long enough to leave detectors undecayed, depending on $\delta_{-} v/x$. For masses within $2m_\mu < m_{A_1^0} < 3m_\pi$ the A_1^0 decays mostly into muon pairs. Like the one from $B \rightarrow K$ decays given in

Eq. (20), this mass range has very tight FCNC constraints (see Sec. IV A 2), but is not ruled out.

The A_1^0 can be searched for with improved measurements of Y decays or $B \rightarrow K$ plus missing energy. The latter needs a high K momentum cut to suppress the $B \rightarrow K \nu \bar{\nu}$ background. For $m_{A_1^0}$ above the Ψ' mass the pseudoscalar can be seen in $b \rightarrow s \tau^+ \tau^-$ decays. The required sensitivity for e.g. the $B \rightarrow X_s \tau^+ \tau^-$ branching ratio is $\mathcal{B}(B \rightarrow X_s \mu^+ \mu^-) m_\tau^2 / m_\mu^2 \lesssim 10^{-3}$.

The NMSSM has different implications for b physics than the MSSM. In particular, the leading log neutral Higgs contribution to radiative $b \rightarrow s \gamma$ and $b \rightarrow s g$ decays is tiny in the latter, but can reach experimental upper limits in the former; see Sec. V A. Furthermore, the MSSM correlation between the $B_s \rightarrow \mu^+ \mu^-$ branching ratio and B_s - \bar{B}_s mixing [39] breaks down due to the additional pseudoscalar. For example, for small $|C_S/C_P|$ the lighter CP -odd Higgs boson dominates the $B_s \rightarrow \mu^+ \mu^-$ rate, which can be anything up to the experimental bound; see Fig. 3. At the same time Δm_s is near its SM value because the leading A_1^0 contribution is independent of the light quark flavor and constrained by Δm_d , and the double penguin from A_2^0 is suppressed. This is in contrast to the MSSM, where a SM-like Δm_s implies an upper bound on $\mathcal{B}(B_s \rightarrow \mu^+ \mu^-)$.

ACKNOWLEDGMENT

G.H. would like to thank Gerhard Buchalla, Yuval Grossman, Howie Haber and Anders Ryd for useful comments, Sven Heinemeyer for FEYNHIGGS support and Bogdan Dobrescu for collaboration at an early stage of this project. G.H. gratefully acknowledges the hospitality of the SLAC theory group.

APPENDIX A: HIGGS SPECTRUM AND COUPLINGS

We give the tree level Higgs spectrum, mixing angles in the minimal flavor and CP violating NMSSM at large $\tan \beta$ and $A_k \ll m_W, x$. The mass matrices in gauge eigenstates can be seen in [9].

The mass eigenstates of the pseudoscalar mixing matrix can be written as

$$\begin{pmatrix} A_1^0 \\ A_2^0 \end{pmatrix} = \begin{pmatrix} \cos \gamma & \sin \gamma \\ -\sin \gamma & \cos \gamma \end{pmatrix} \begin{pmatrix} A^0 \\ N_I \end{pmatrix} \tag{A1}$$

where $N_I = \text{Im } N / \sqrt{2}$, $A^0 = \sqrt{2}(\sin \beta \text{Im } H_d^0 + \cos \beta \text{Im } H_u^0)$ and the Goldstone boson is given as $G^0 = \sqrt{2}(\cos \beta \text{Im } H_d^0 - \sin \beta \text{Im } H_u^0)$. The mixing angle and masses read as

$$\gamma = \frac{\pi}{2} + \frac{v}{x \tan \beta} \delta_- + \mathcal{O}\left(\frac{1}{\tan^2 \beta}\right),$$

$$\text{i.e. } \sin \gamma \approx 1, \cos \gamma \approx -\frac{v}{x \tan \beta} \delta_- \tag{A2}$$

and

$$m_{A_1^0}^2 = 3kx A_k, \quad m_{A_2^0}^2 = m_A^2 \tag{A3}$$

where we defined

$$\delta_{\mp} = \frac{A_{\lambda \mp} 2kx}{A_{\lambda} + kx} \tag{A4}$$

and m_A^2 is given in Eq. (16).

The scalar mass matrix can be diagonalized analytically in the large $\tan \beta$ limit by first decoupling the heaviest state and then rotating the remaining 2×2 block by the angle θ along the lines of Ref. [21]. The result can be written as

$$\begin{pmatrix} h^0 \\ H_1^0 \\ H_2^0 \end{pmatrix} = \sqrt{2} \begin{pmatrix} \frac{1}{\tan \beta} \left(\cos \theta - \frac{v}{x} \delta_+ \sin \theta \right) & \cos \theta & -\sin \theta \\ \frac{1}{\tan \beta} \left(\sin \theta + \frac{v}{x} \delta_+ \cos \theta \right) & \sin \theta & \cos \theta \\ 1 & \frac{-1}{\tan \beta} & \frac{-v}{x \tan \beta} \delta_+ \end{pmatrix} \begin{pmatrix} \text{Re } H_d^0 - v_d \\ \text{Re } H_u^0 - v_u \\ \text{Re } N - x \end{pmatrix} \tag{A5}$$

with the mixing angle and scalar masses

$$\tan 2\theta = \frac{4\lambda^2 v x}{4k^2 x^2 - m_Z^2} \tag{A6}$$

$$m_{H_2^0}^2 = m_A^2, \quad m_{h^0, H_1^0}^2 = \frac{1}{2} [4k^2 x^2 + m_Z^2 \mp \sqrt{(4k^2 x^2 - m_Z^2)^2 + 16\lambda^4 x^2 v^2}]. \tag{A7}$$

The mass of the charged Higgs boson is given as

$$m_{H^\pm}^2 = m_A^2 + m_W^2 - \lambda^2 v^2. \tag{A8}$$

Feynman rules

Feynman rules can be read off the Lagrangians given at leading order in $\tan \beta$. Note that $A_2^0 \approx -A_{MSSM}^0$ in this limit. Couplings to up (u) and down (d) type fermions:

$$\mathcal{L}_{A_i^0 \bar{d}d} = -i \frac{gm_d}{2m_W} \left(\frac{v}{x} \delta_{-A_1^0, \tan \beta A_2^0} \right) \bar{d} \gamma_5 d, \quad (\text{A9})$$

$$\mathcal{L}_{A_i^0 \bar{u}u} = -i \frac{gm_u}{2m_W} \frac{1}{\tan \beta} \left(\frac{v}{x \tan \beta} \delta_{-A_1^0, A_2^0} \right) \bar{u} \gamma_5 u, \quad (\text{A10})$$

$$\begin{aligned} \mathcal{L}_{(h^0, H_i^0) \bar{d}d} = & -\frac{gm_d}{2m_W} \left(\left(\cos \theta - \frac{v}{x} \delta_+ \sin \theta \right) h^0, \right. \\ & \left. \times \left(\sin \theta + \frac{v}{x} \delta_+ \cos \theta \right) H_1^0, \tan \beta H_2^0 \right) \bar{d}d, \end{aligned} \quad (\text{A11})$$

$$\mathcal{L}_{(h^0, H_i^0) \bar{u}u} = -\frac{gm_u}{2m_W} \left(\cos \theta h^0, \sin \theta H_1^0, -\frac{H_2^0}{\tan \beta} \right) \bar{u}u. \quad (\text{A12})$$

Couplings to charginos:

$$\mathcal{L}_{A_1^0 \chi^+ \chi^-} = +i \frac{\lambda}{\sqrt{2}} A_1^0 \bar{\chi}_i^+ [U_{i2} V_{j2} L - U_{j2} V_{i2} R] \chi_j^- \quad (\text{A13})$$

where $L, R = (1 \mp \gamma_5)/2$ are chiral projectors.

APPENDIX B: CONVENTIONS, LOOP FUNCTIONS

The chargino mass matrix is written as ($\mu_{MSSM} = -\lambda x$)

$$M_{\chi^\pm} = \begin{pmatrix} m_2 & \sqrt{2} m_W \sin \beta \\ \sqrt{2} m_W \cos \beta & -\lambda x \end{pmatrix}. \quad (\text{B1})$$

It is diagonalized by the orthogonal matrices U, V (we do not include beyond CKM *CP* violation):

$$UM_{\chi^\pm} V^T = \text{diag}(m_{\chi_1}, m_{\chi_2}). \quad (\text{B2})$$

The stop mixing matrix is given as

$$\begin{pmatrix} \tilde{t}_1 \\ \tilde{t}_2 \end{pmatrix} = \begin{pmatrix} \cos \theta_t^- & \sin \theta_t^- \\ -\sin \theta_t^- & \cos \theta_t^- \end{pmatrix} \begin{pmatrix} \tilde{t}_L \\ \tilde{t}_R \end{pmatrix}. \quad (\text{B3})$$

Here, $\tilde{t}_{1,2}$ are the mass and $\tilde{t}_{L,R}$ the gauge eigenstates.

The loop functions are defined as

$$D_2(x, y) = \frac{x \ln x}{(1-x)(x-y)} + (x \leftrightarrow y), \quad D_2(1, 1) = -\frac{1}{2}, \quad (\text{B4})$$

$$D_3(x) = \frac{x \ln x}{1-x}, \quad D_3(1) = -1. \quad (\text{B5})$$

APPENDIX C: DECAY RATES

The rate of the light NMSSM pseudoscalar into down-type fermions is given as

$$\Gamma(A_1^0 \rightarrow \bar{f}f) = \frac{1}{4\pi} \frac{G_F}{\sqrt{2}} \left(\frac{v}{x} \delta_- \right)^2 m_{A_1^0} m_f^2 \sqrt{1 - 4 \frac{m_f^2}{m_{A_1^0}^2}} r \quad (\text{C1})$$

where $r=1$ for leptons and $r=N_C$ for quarks. The decay rate into up quarks is $1/\tan^4 \beta$ suppressed. The rate into two photons reads as

$$\Gamma(A_1^0 \rightarrow \gamma\gamma) = \frac{\alpha^2}{8\pi^3} \frac{G_F}{\sqrt{2}} m_{A_1^0}^3 \left| \sum_i I_i \right|^2 \quad (\text{C2})$$

where for $i=e, \mu, \tau$ and d, s, b loops $I_i = r Q_i^2 \kappa_i F(\kappa_i) \delta_{-v/x}$, $\kappa_i = m_i^2/m_{A_1^0}^2$ and Q_i is the charge of the fermion. The function $F(\kappa)$ can be seen in [40]. It assumes the limits

$$\kappa F(\kappa) = \begin{cases} 0 & \text{for } \kappa \ll 1, \\ -\frac{1}{2} & \text{for } \kappa \gg 1, \\ -\frac{\pi^2}{8} & \text{for } \kappa = \frac{1}{4}. \end{cases} \quad (\text{C3})$$

Higgsino loops contribute as $I_{\tilde{\chi}} = \sqrt{2} U_{i2} V_{i2} \lambda m_W / m_{\tilde{\chi}} \kappa_{\tilde{\chi}} F(\kappa_{\tilde{\chi}})$. It follows from Eq. (C3) that near $m_{A_1^0} \leq 2m_\mu$ the $\gamma\gamma$ rate is dominated by the muon loop. Contributions from up-type quarks are suppressed by $1/\tan^4 \beta$.

The decay rates for inclusive and exclusive $b \rightarrow s A_1^0$ FCNCs read as

$$\Gamma(B \rightarrow X_s A_1^0) = \frac{G_F^2 |V_{tb} V_{ts}^*|^2}{2^{10} \pi^5} |C_A|^2 \frac{(m_b^2 - m_{A_1^0}^2)^2}{m_b^3}, \quad (\text{C4})$$

$$\begin{aligned} \Gamma(B \rightarrow K A_1^0) = & \frac{G_F^2 |V_{tb} V_{ts}^*|^2}{2^{10} \pi^5} |C_A|^2 \frac{|\vec{p}_K|^2}{m_B^2} |f_0(m_A^2)|^2 \\ & \times \left(\frac{m_B^2 - m_K^2}{m_b} \right)^2, \end{aligned} \quad (\text{C5})$$

where the form factor f_0 parametrizes the matrix element

$$\langle K(p_K) | \bar{s}_L b_R | B(p_B) \rangle = \frac{1}{2} \left(\frac{m_B^2 - m_K^2}{m_b} \right) f_0 ((p_B - p_K)^2). \quad (\text{C6})$$

Here, \vec{p}_K denotes the three momentum of the kaon and $f_0(0) \sim 0.3-0.4$ [35].

The branching ratio for radiative Υ decays is given as, e.g., [18],

$$\frac{\mathcal{B}(\Upsilon \rightarrow A_1^0 \gamma)}{\mathcal{B}(\Upsilon \rightarrow \mu^+ \mu^-)} = \frac{G_F m_Y^2}{4\sqrt{2}\pi\alpha} \left(\frac{v}{x} \delta_- \right)^2 \left(1 - \frac{m_{A_1^0}^2}{m_Y^2} \right) F \quad (\text{C7})$$

where $F \sim 1/2$ includes QCD corrections and $\mathcal{B}(\Upsilon(1s) \rightarrow \mu^+ \mu^-) = (2.48 \pm 0.06)\%$ [31].

-
- [1] S.R. Choudhury and N. Gaur, Phys. Lett. B **451**, 86 (1999); K.S. Babu and C.F. Kolda, Phys. Rev. Lett. **84**, 228 (2000); M. Carena, D. Garcia, U. Nierste, and C.E.M. Wagner, Nucl. Phys. **B577**, 88 (2000).
- [2] C.S. Huang, W. Liao, Q.S. Yan, and S.H. Zhu, Phys. Rev. D **63**, 114021 (2001); **64**, 059902(E) (2001).
- [3] C. Bobeth, T. Ewerth, F. Kruger, and J. Urban, Phys. Rev. D **64**, 074014 (2001).
- [4] A.J. Buras, P.H. Chankowski, J. Rosiek, and L. Slawianowska, Nucl. Phys. **B619**, 434 (2001); A. Dedes and A. Pilaftsis, Phys. Rev. D **67**, 015012 (2003); A. Dedes, Mod. Phys. Lett. A **18**, 2627 (2003).
- [5] G. Isidori and A. Retico, J. High Energy Phys. **11**, 001 (2001).
- [6] A.J. Buras, P.H. Chankowski, J. Rosiek, and L. Slawianowska, Nucl. Phys. **B659**, 3 (2003).
- [7] G. Hiller and F. Krüger, Phys. Rev. D **69**, 074020 (2004).
- [8] H.P. Nilles, M. Srednicki, and D. Wyler, Phys. Lett. **120B**, 346 (1983); J.M. Frere, D.R.T. Jones, and S. Raby, Nucl. Phys. **B222**, 11 (1983); J.P. Derendinger and C.A. Savoy, *ibid.* **B237**, 307 (1984).
- [9] J.R. Ellis, J.F. Gunion, H.E. Haber, L. Roszkowski, and F. Zwirner, Phys. Rev. D **39**, 844 (1989).
- [10] B.A. Dobrescu and K.T. Matchev, J. High Energy Phys. **09**, 031 (2000).
- [11] B.A. Dobrescu, Phys. Rev. D **63**, 015004 (2001).
- [12] B.A. Dobrescu, G. Landsberg, and K.T. Matchev, Phys. Rev. D **63**, 075003 (2001); U. Ellwanger, J.F. Gunion, C. Hugonin, and S. Moretti, *ibid.* **63**, 075003 (2001).
- [13] U. Ellwanger, M. Rausch de Traubenberg, and C.A. Savoy, Nucl. Phys. **B492**, 21 (1997).
- [14] B. Ananthanarayan and P.N. Pandita, Phys. Lett. B **353**, 70 (1995); **371**, 245 (1996); Int. J. Mod. Phys. A **12**, 2321 (1997).
- [15] T. Han, D. Marfatia, and R.J. Zhang, Phys. Rev. D **61**, 013007 (2000).
- [16] R. Kitano, G.D. Kribs, and H. Murayama, hep-ph/0402215.
- [17] J.M. Frere, J.A.M. Vermaseren, and M.B. Gavela, Phys. Lett. **103B**, 129 (1981); L.J. Hall and M.B. Wise, Nucl. Phys. **B187**, 397 (1981); B. Grzadkowski and P. Krawczyk, Z. Phys. C **18**, 43 (1983); S. Bertolini, F. Borzumati, and A. Masiero, Nucl. Phys. **B312**, 281 (1989); C. Bird, P. Jackson, R. Kowalewski, and M. Pospelov, hep-ph/0401195.
- [18] H.E. Haber, A.S. Schwarz, and A.E. Snyder, Nucl. Phys. **B294**, 301 (1987).
- [19] J. Rosiek, hep-ph/9511250.
- [20] F. Franke and H. Fraas, Int. J. Mod. Phys. A **12**, 479 (1997).
- [21] D.J. Miller, R. Nevzorov, and P.M. Zerwas, Nucl. Phys. **B681**, 3 (2004).
- [22] U. Ellwanger, Phys. Lett. B **303**, 271 (1993); P.N. Pandita, *ibid.* **318**, 338 (1993); Z. Phys. C **59**, 575 (1993); T. Elliott, S.F. King, and P.L. White, Phys. Lett. B **314**, 56 (1993); Phys. Rev. D **49**, 2435 (1994).
- [23] CLEO Collaboration, R. Ammar *et al.*, Phys. Rev. Lett. **87**, 271801 (2001).
- [24] BABAR Collaboration, B. Aubert *et al.*, hep-ex/0304020.
- [25] BABAR Collaboration, B. Aubert *et al.*, hep-ex/0308016.
- [26] Belle Collaboration, J. Kaneko *et al.*, Phys. Rev. Lett. **90**, 021801 (2003).
- [27] Belle Collaboration, A. Ishikawa *et al.*, Phys. Rev. Lett. **91**, 261601 (2003).
- [28] BABAR Collaboration, B. Aubert *et al.*, Phys. Rev. Lett. **91**, 221802 (2003).
- [29] E865 Collaboration, R. Appel *et al.*, Phys. Rev. Lett. **83**, 4482 (1999).
- [30] E787 Collaboration, S. Adler *et al.*, Phys. Lett. B **537**, 211 (2002); E787 Collaboration, hep-ex/0403034.
- [31] Particle Data Group Collaboration, K. Hagiwara *et al.*, Phys. Rev. D **66**, 010001 (2002).
- [32] CLEO Collaboration, T.E. Coan *et al.*, Phys. Rev. Lett. **80**, 1150 (1998); updated in A. Kagan, hep-ph/9806266.
- [33] Y. Grossman, Z. Ligeti, and E. Nardi, Phys. Rev. D **55**, 2768 (1997).
- [34] CDF Collaboration, D. Acosta *et al.*, hep-ex/0403032.
- [35] A. Ali, P. Ball, L.T. Handoko, and G. Hiller, Phys. Rev. D **61**, 074024 (2000).
- [36] CLEO Collaboration, R. Balest *et al.*, Phys. Rev. D **51**, 2053 (1995).
- [37] F. Borzumati, C. Greub, T. Hurth, and D. Wyler, Phys. Rev. D **62**, 075005 (2000).
- [38] <http://www.feynhiggs.de>; S. Heinemeyer, Eur. Phys. J. C **22**, 521 (2001); M. Frank, S. Heinemeyer, W. Hollik, and G. Weiglein, hep-ph/0212037.
- [39] A.J. Buras, P.H. Chankowski, J. Rosiek, and L. Slawianowska, Phys. Lett. B **546**, 96 (2002).
- [40] J.F. Gunion, G. Gamberini, and S.F. Novaes, Phys. Rev. D **38**, 3481 (1988).